

# Application of Low- and Mid-Frequency Raman Spectroscopy to Characterize the Amorphous-Crystalline Transformation of Indomethacin

Peter J. Larkin,<sup>a,\*</sup> John Wasylyk,<sup>a,†</sup> Michaella Raglione<sup>b,‡</sup>

<sup>a</sup> Bristol-Myers Squibb Company, New Brunswick, NJ 08903 USA

<sup>b</sup> University of Delaware, Newark, DE 19716 USA

Raman spectroscopy using the mid-frequency (1800–1500 cm<sup>-1</sup>) and low-frequency (200–8 cm<sup>-1</sup>) spectral regions is used to study the transformation of amorphous indomethacin (IND) to the  $\gamma$ -crystalline form. The low-frequency spectral region provides access to collective vibrations of molecules in the crystalline and amorphous state, while the mid-frequency spectral region provides access to the molecular vibrations that are sensitive to the local functional group environment. Both spectral regions provide distinct Raman bands for the amorphous and crystalline forms of IND. The more intense low-frequency Raman bands provide greater sensitivity for detecting the onset of crystallization in an amorphous matrix. Subtle differences in the behavior of the initial crystalline process of IND are observed between the low-frequency and mid-frequency Raman bands. These observations suggest that different responses for mid- and low-frequency Raman bands occur for the microcrystalline domains present during the initial crystallization process. The suitability of low-frequency Raman spectroscopy to monitor IND in a suspension was demonstrated. This suggests that the technique will be a valuable tool for at-line and on-line monitoring of active pharmaceutical ingredient crystallization.

Index Headings: **Raman; Mid-frequency; Low frequency; Crystallization; Crystalline form; Amorphous form; Indomethacin.**

## INTRODUCTION

Active pharmaceutical ingredients (APIs) often exist in several different solid-state forms and can undergo transformations between the various forms with consequences for the effectiveness of the drug product.<sup>1</sup> In general, amorphous APIs are thermodynamically unstable and will eventually crystallize into the more energetically favored form.<sup>1,2</sup> Crystallizations from the amorphous form are affected by a number of factors, including temperature and humidity.<sup>3</sup> Amorphous material lacks the long-range order characteristic of crystalline materials but can include short-range orientational and positional order.<sup>2</sup> Typically, the amorphous form exhibits enhanced dissolution rates and solubility in comparison with the API's crystalline counterparts.<sup>4</sup> However, crystalline forms are often thermodynamically

favored, resulting in poor solid-state form stability of the amorphous API.

Vibrational spectroscopic techniques can provide a probe of molecular structure and local environments, thereby affording valuable insight into both the amorphous and crystalline states of molecular substances such as APIs. Techniques such as mid-infrared, near-infrared, and Raman spectroscopies are employed because of their attributes that include non-destructive sampling, spectral specificity for the solid-state form, as well as the ability to identify and quantitate components in complex mixtures.<sup>5</sup> This has made vibrational spectroscopy an attractive choice to identify and determine the crystallinity of API solid-state forms.

Raman spectroscopy is characterized by much narrower bandwidths than either mid-infrared or near-infrared spectroscopy.<sup>6</sup> This is an important factor in the excellent specificity Raman spectroscopy exhibits for the various solid-state forms of APIs. Many of the APIs used in drug products contain aromatic moieties, and in most cases, pharmaceutical excipients do not contain any aromatic moieties. Typically, the Raman bands of aromatic APIs are more intense than those observed for their saturated aliphatic excipient counterparts, resulting in enhanced sensitivity for the API in drug product formulations.<sup>7</sup> Raman spectroscopy has been used to monitor API solid-state transformations during processing operations, evaluate crystal form stability, and investigate model dissolution process to understand the API transformation kinetics under varying experimental conditions.<sup>8,9</sup> Recent technological advances facilitate Raman measurements to more easily include the low-frequency spectral region, which significantly improves the solid-state specificity for API form.<sup>10</sup> The low-frequency region provides access to the lattice vibrations of molecular crystals and, as a result, provides more direct monitoring of the intermolecular interactions in the solid state.<sup>11,12</sup> The Raman bands in the 200–100 cm<sup>-1</sup> region can include contributions from selected molecular vibrations such as out-of-plane aromatic ring deformations.<sup>7</sup> The lowest-frequency Raman bands below 100 cm<sup>-1</sup> are more likely to involve more purely phonon (lattice) vibrational modes of the crystalline lattice.<sup>13,14</sup> The low-frequency Raman spectral region can also provide some information on the short-range order that may exist in solution or in the solid amorphous state. Thus, the Raman spectrum that includes both the standard spectral region (4000–200 cm<sup>-1</sup>) and the low-frequency spectral region (200–8 cm<sup>-1</sup>) provides bands related to both the local environment of the molecules, as

Received 24 February 2015; accepted 29 July 2015.

\* Current address: Cytec Industries, 1937 West Main Street, Stamford, CT 06902

† Author to whom correspondence should be sent. E-mail: john.wasylyk@bms.com.

‡ Summer intern student

DOI: 10.1366/15-07926

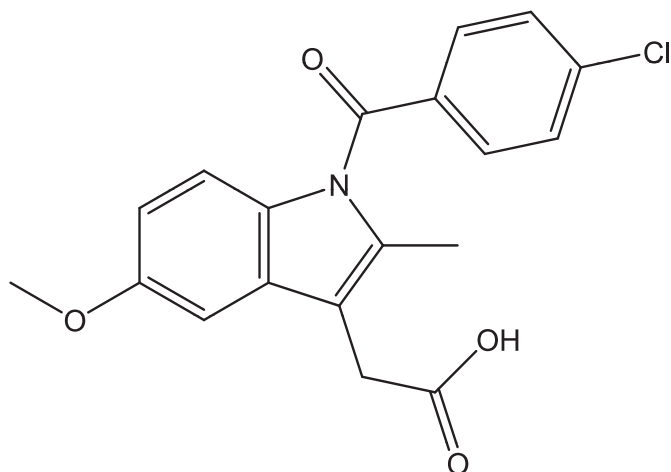


Fig. 1. Chemical structure of IND.

well as the larger crystalline lattice environment, and can provide a discriminating probe of the crystallization process.<sup>15</sup>

Crystalline and amorphous indomethacin (IND) has been used by a number of authors as a model system to study API crystallization mechanisms and kinetics.<sup>16–18</sup> Various techniques have been used to characterize the different solid-state forms of IND, including Raman spectroscopy.<sup>19,20</sup> Indomethacin, shown in Fig. 1, is an indole acetic acid derivative that is used as a non-steroidal, anti-inflammatory agent. The three reported crystalline forms ( $\gamma$ -form,  $\alpha$ -form, and  $\delta$ -form) are considered to be poorly water soluble, resulting in low bioavailability. Enhanced solubility and dissolution properties are observed for the amorphous form of IND.<sup>21,22</sup> Amorphous IND is not thermodynamically favored, and conversion to the more stable crystalline forms can readily occur.<sup>18,20</sup> Typically, amorphous IND can be prepared either by melting followed by rapid quench cooling or by milling and grinding.<sup>17,18</sup>

The amorphous and  $\gamma$ -forms of IND have been studied using theoretical calculations of individual and molecular dimers, and these results have been correlated to the infrared (IR) and Raman spectra. These studies confirmed that quench-cooled amorphous IND consists primarily of carboxylic acid dimers similar in structure to what is observed in  $\gamma$ -crystalline form.<sup>23,24</sup> The mid-frequency region between 1800–1500  $\text{cm}^{-1}$  provides strong IR and Raman bands involving the carboxylic acid and the benzoyl amide carbonyl stretches, respectively.<sup>16,17,19,20,23</sup> Both carbonyl groups have bands that occur between 1740–1660  $\text{cm}^{-1}$  and have been used to understand the amorphous-crystalline IND transformation. Their carbonyl frequencies are dependent upon the local molecular environment of the crystalline and amorphous IND forms. The Raman spectrum of IND provides distinctive bands for the amorphous and  $\gamma$ -form. The bands occurring between 1650–1550  $\text{cm}^{-1}$  involve in-plane stretching vibrations of the substituted indole and para-substituted aryl group and provide distinctive bands for the amorphous and crystalline forms.<sup>6</sup> Low-frequency Raman spectroscopy has also been used to study the IND crystallization process and kinetics, which

demonstrated the high sensitivity of the low-frequency Raman spectral region in comparison to the diagnostic carbonyl stretching bands in the mid-frequency Raman spectral region.<sup>20</sup>

An investigation of the amorphous-crystalline transformation of IND was performed using both the mid-frequency (1800–1500  $\text{cm}^{-1}$ ) and the low-frequency range (200–100  $\text{cm}^{-1}$ ). The amorphous IND was prepared by melting, followed by rapid quench cooling, and the subsequent transformation to the  $\gamma$ -form was monitored by Raman spectroscopy. A Kaiser RXN1 Raman spectrometer was employed and interfaced to an Ondax XLF-CLM Raman sampling system in order to measure the full Raman spectrum from 3500–8  $\text{cm}^{-1}$ . This was done to enable monitoring of both the standard fingerprint region and low-frequency Raman spectral regions simultaneously. Significant differences in the initial phase of the crystallization process of IND between the mid- and low-frequency Raman data were observed. This suggests that the two spectral regions provide different probes into the microcrystalline domains present in the initial crystallization process. As IND becomes more highly crystalline, both spectral regions give analogous results. The concentration dependence of the Raman spectrum of IND was studied in both solution and as a suspension to demonstrate the feasibility for both an at- and on-line analytical technique to monitor API crystallization.

## EXPERIMENTAL

**Materials.** Indomethacin was purchased from Sigma-Aldrich (lot MLBR4530V), and its  $\gamma$ -crystalline form was confirmed using powder X-ray diffraction (PXRD). Amorphous IND was prepared by placing the white crystalline powdered API on a microscope slide, heating on a hot plate until melted ( $\sim 170$  °C), and quench cooling in dry ice, resulting in a yellow, amorphous solid. Indomethacin, dissolved in ethanol or chloroform, also exhibited the same yellow color. The amorphous form of IND was confirmed by PXRD and was found to be stable when stored in a capped glass vial at 8 °C over a two-month time period. Conversion to the thermodynamically favored crystalline form occurs at room temperature. Successful preparation of the  $\alpha$  and  $\gamma$  IND crystalline forms was confirmed by PXRD.

**Instrumentation.** The low-frequency Raman spectra were measured using 785.64 nm excitation, 180° back-scattering geometry, and a spectral range that included both the Stokes and the anti-Stokes scattering from –39 to 3467  $\text{cm}^{-1}$ . The instrument components included a Kaiser Optical Systems, Inc. Raman RXN1 Analyzer spectrograph with a f/1.8 axial transmission imaging spectrograph which employed a HoloPlex transmission grating (HDG-785.1, 0.05  $\text{cm}^{-1}$ /pixel, Kaiser Optical Systems, Inc.) with an entrance slit width of 50  $\mu\text{m}$  (SLIT-50) and a thermoelectrically cooled 1024  $\times$  256 element charge-coupled device (CCD) detector (Andor CC-001). The single-stage spectrograph was interfaced via a 25  $\mu\text{m}$  diameter 0.1 numerical aperture (NA) step index (HJPSC25, ThorLabs) optical fiber to an XLF-CLM Raman sampling system (Ondax) that included a Sure-Lock 785 nm wavelength stabilized laser diode and a

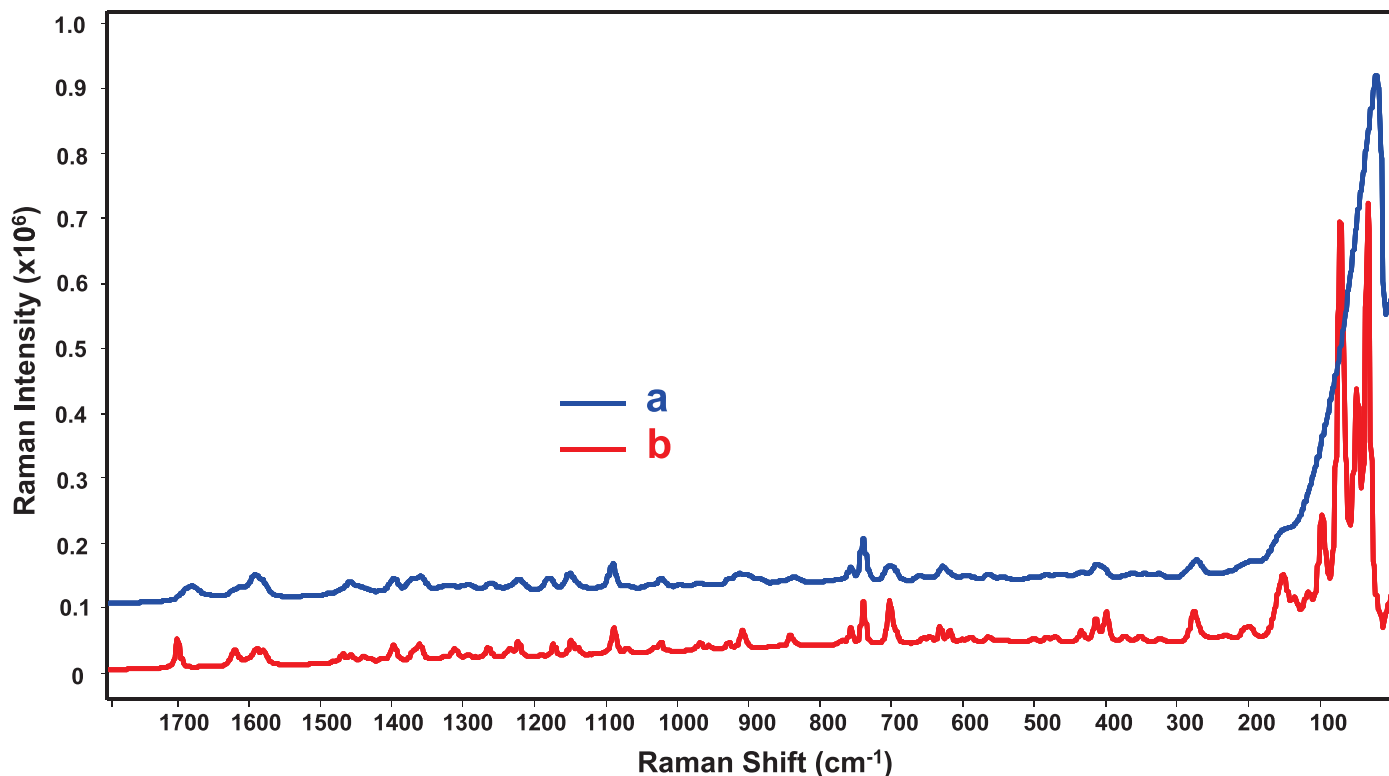


Fig. 2. Mid-frequency and low-frequency Raman spectra of the (a) blue, amorphous and (b) red,  $\gamma$ -form of IND. Significant differences are observed between the amorphous and crystalline state in both the high- and low-frequency spectral regions. The excellent specificity for crystalline material and the significant increased intensity in the low-frequency region is clearly observed.

SureBlock XLF notch filter system arranged to collect  $180^\circ$  backscattered radiation from the IND solution, suspension, and powdered samples contained in borosilicate glass vials (VWR, part number 470 206-388). Data acquisition was made using HoloGrams v4.1 and HoloReact v2.0.0.0 (Kaiser Optical Systems, Inc.) and included both a dark subtraction and cosmic ray filter. The solutions, suspensions, and powdered samples were measured using an exposure of 1000 ms and 25 accumulations for a total measurement time of 50 s. The conversion of the amorphous IND to crystalline material over seven days utilized a longer, 10 min measurement time using 5 s and 60 accumulations.

Powder X-ray diffraction (PXRD) analysis measurements were used to confirm the IND crystalline form and to confirm that the preparation of amorphous material was free of crystalline impurities. The PXRD analysis was measured at room temperature using a D8 Advance (Bruker) equipped with a manual  $\chi$  platform goniometer and Vantec 500 detector with Cu  $K\alpha$  radiation at wavelength 1.5418 Å. The samples were placed in glass capillaries of 0.7 mm in diameter and rotated during the data collection to minimize preferred orientation. The data was collected between  $2^\circ$  and  $32^\circ$   $2\theta$  and integrated with a step size of  $0.04^\circ$  and a sample exposure time of 300 s.

**Software.** The Raman data were converted to the GRAMS format (\*.SPC) and were analyzed using GRAMS/AI 7.02 (Thermo Scientific) and Excel 2007 (Microsoft). The scatter plots and regression analysis were prepared using SigmaPlot 13.0 (Systat Software, Inc.). All spectral data were collected using HoloReact

v2.0.0.0 (Kaiser Optical Systems, Inc.) including preprocessing and waterfall plot displays.

## RESULTS AND DISCUSSION

**Comparison of Conventional and Low-Frequency Raman Spectra of Crystalline and Amorphous Indomethacin.** The Raman spectra of the amorphous and  $\gamma$ -forms of IND plotted from 1800 to  $8\text{ cm}^{-1}$  are shown in Fig. 2. The spectra were acquired on a single-stage imaging spectrograph that collects the entire spectral region in a single scan. The wavelength axes of the two fingerprint regions are expanded to facilitate comparison of the spectral features. As discussed in previous work, the Raman intensity of the low-frequency region of aromatic APIs are typically tenfold greater than the most intense Raman bands in the classic fingerprint region ( $2000\text{--}400\text{ cm}^{-1}$ ).<sup>7</sup> The Raman spectra in Fig. 2 of IND demonstrate this same behavior.

In general, the infrared and Raman spectra of amorphous materials are characterized by broader, less distinct bands than are observed for the crystalline forms of the same molecular species.<sup>8</sup> Amorphous material, strictly defined, lacks long-range order and exhibits only the short-range order typical of liquids.<sup>1,2</sup> Conversely, crystalline forms are composed of molecules arranged in a three-dimensional structure with a local pattern that is repeated periodically in all directions resulting in a well-defined lattice.<sup>1</sup> The amorphous definitions of APIs are often extended to also include disordered crystalline and microcrystalline solids.<sup>2</sup> The Raman spectrum of amorphous IND shown in Fig. 2 shows broadening, and

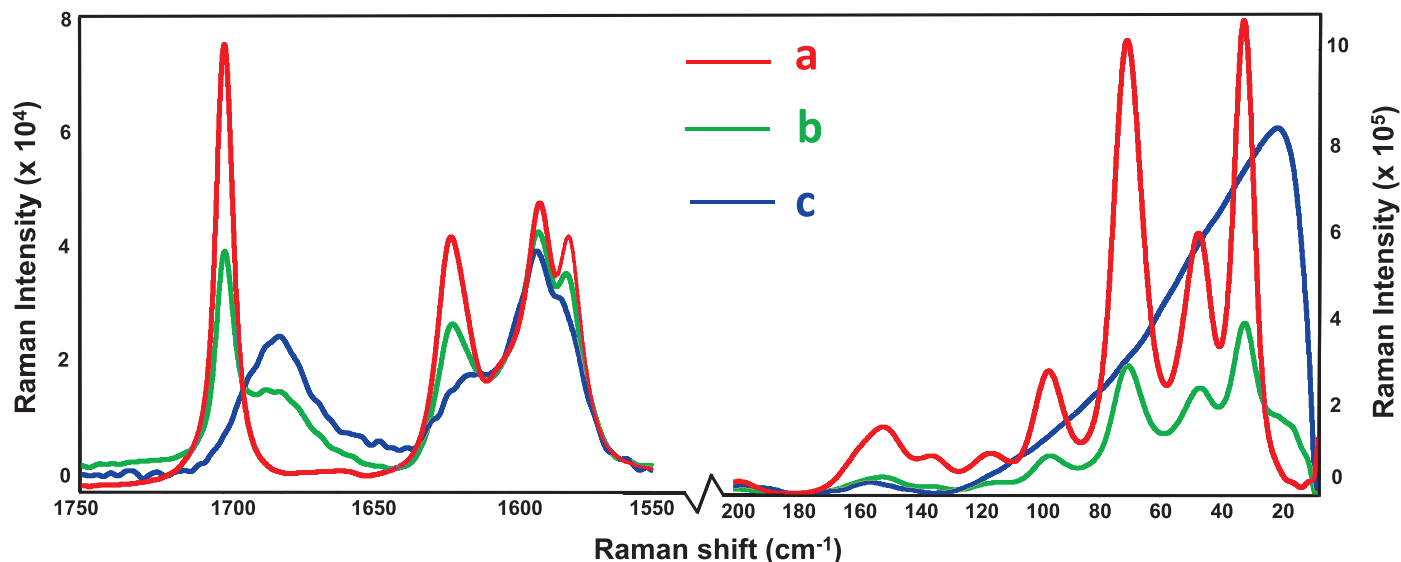


FIG. 3. Raman spectra of (a) red, fully crystalline  $\gamma$ -form, (b) green, an equal mixture ( $\sim 50/50$ ) of  $\gamma$ -crystalline–amorphous IND, and (c) blue, the fully amorphous IND. The two spectral regions include the mid-frequency region ( $1750\text{--}1550\text{ cm}^{-1}$ ) that includes the carbonyl stretching bands and the low-frequency spectral region ( $200\text{--}8\text{ cm}^{-1}$ ). Because the Raman band intensities are tenfold greater in the low-frequency region, the spectra in each region are normalized using the most intense  $\gamma$ -form Raman band ( $1699$  and  $32\text{ cm}^{-1}$ ) to facilitate visualization of both spectral regions.

frequency shifts of bands in comparison with the  $\gamma$ -crystalline form ( $\gamma$ -form) in all spectral regions. The spectral characteristics of the amorphous material can be attributed to a range of molecular conformations and intermolecular bonding arrangements. This is particularly pronounced in the low-frequency spectral region where a broad intense band, which derives from the vibrational density of states (VDOS), the Boson peak, and inelastically scattered radiation is observed in the amorphous form of IND.<sup>14,20,25</sup> The sharp, intense low-frequency Raman bands of the  $\gamma$ -form of IND result from contributions generated not only from selected molecular vibrations but also crystalline lattice vibrational modes. For aromatic molecules typical of APIs, the low-frequency molecular vibrations, including aromatic ring out-of-plane bending modes and substituent torsional modes, are generally observed between  $200\text{--}100\text{ cm}^{-1}$ .<sup>7,13</sup> The crystal lattice vibrations which involve movement of the entire molecular species with respect to each other within the crystalline solid are typically encountered below  $100\text{ cm}^{-1}$  for aromatic compounds.<sup>13</sup> The presence of the Boson peak at  $21\text{ cm}^{-1}$  in amorphous IND indicates that some short-range order information is also available in the low-frequency Raman spectral region. Differentiation between the crystalline and amorphous phases is clearly demonstrated in the Raman spectra of IND shown in Fig. 2. Previous work has demonstrated that the mid-frequency IR and Raman spectra as well as the low-frequency Raman spectrum can be used to characterize the amorphous and crystalline components of IND.<sup>15,19,21,23</sup> Much of the mid-frequency–based IR and Raman work focused on the spectral region between  $1800$  and  $1500\text{ cm}^{-1}$ .

**Amorphous to Crystalline Indomethacin Transformation.** Figure 3 shows both the selected mid-frequency ( $1750\text{--}1550\text{ cm}^{-1}$ ) and the low-frequency Raman spectral regions of the  $\gamma$ -form, the amorphous, and a nominally

equal mixture of the two phases ( $50/50$ ) of IND. The two spectral regions are normalized to the intensity of the strongest peaks in each spectral region to facilitate comparison of both the selected mid-frequency and low-frequency spectral features. This normalization results in a tenfold expansion of the Raman intensity in the carbonyl region relative to the low-frequency Raman intensity. As shown in Fig. 3, unique spectral features for both the amorphous and crystalline IND phases are observed in both the mid- and the low-frequency Raman spectral regions. The assignments for the mid-frequency IR and Raman bands along with some of the more prominent low-frequency Raman bands are summarized in Table I.

The carbonyl stretch of the carboxylic acid dimer has negligible intensity in the Raman spectrum.<sup>16,19,21</sup> The substitution of the benzoyl carbonyl on the nitrogen atom of indole-aromatic ring and the para-substituted aromatic group in the IND molecule result in  $\pi$  orbital interaction and significant Raman intensity for this carbonyl stretch.<sup>26</sup> The amorphous IND benzoyl tertiary amide carbonyl stretch occurs at  $1681\text{ cm}^{-1}$  and has a full width half-height (FWHH) of  $25\text{ cm}^{-1}$ . In the case of the  $\gamma$ -form, the carbonyl band occurs at  $1699\text{ cm}^{-1}$  and has a FWHH only  $7\text{ cm}^{-1}$ . When IND is in the  $\gamma$ -form, this benzoyl amide carbonyl group is stacked in close proximity, resulting in very different bandwidths and frequencies than in the amorphous state.<sup>23</sup> Adjacent to the strong Raman band from the benzoyl amide carbonyl group are the quadrant stretching bands involving the para-substituted aromatic and the substituted indole ring.<sup>6,23</sup> The  $\gamma$ -form of IND is characterized by a sharp Raman band at  $1621\text{ cm}^{-1}$  (FWHH  $12\text{ cm}^{-1}$ ) that broadens and shifts to the lower frequency of  $1612\text{ cm}^{-1}$  (FWHH  $22\text{ cm}^{-1}$ ) for the amorphous species.

The Raman spectrum of amorphous IND is characterized by a broad, asymmetric band in the low-frequency region with a maximum at  $21\text{ cm}^{-1}$  and a FWHH of

**TABLE I. Selected infrared and Raman peak positions and band assignments for indomethacin. The spectral regions include 1750–1550 cm<sup>-1</sup> and below 100 cm<sup>-1</sup>.**

Functional group	Crystalline $\gamma$ -form			Amorphous IND			Band assignments <sup>d</sup>
	Bands (cm <sup>-1</sup> ) <sup>a</sup>		FWHH (cm-1)	Bands (cm <sup>-1</sup> )		FWHH (cm-1)	
	IR <sup>b</sup>	Raman		IR <sup>b</sup>	Raman		
Carboxylic acid <sup>c</sup>				1735 (sh)			Non-Hydrogen bonded COOH asymmetric C=O str. Hydrogen bonded COOH dimer asymmetric C=O str.
Benzoyl carbonyl	1716 (s)		7	1709 (s)			C=O str.
Indole ring	1692 (s)	1699 (s)	12	1682 (s)	1681 (s)	25	Involves the aryl ring quadrant str.
Chloro benzene	1612 (m)	1620 (s)	10	1610 (m)	1612 (s)	22	Involves the aryl ring quadrant str.
	1579 (m)	1579 (m)	5	1580 (m)	1582 (m)	15	Involves chloro benzene Aryl ring quadrant str.
	1589 (m)	1589 (m)	7	1591 (m)	1590 (m)	11	
		70 (vs)	9.5				
		47 (vs)	6				
		32 (vs)	8				
				21 (vs)		50	Lattice-phonon vibration Boson

<sup>a</sup> IR and Raman intensities: vs = very strong; s = strong; m = medium; sh = shoulder. The Raman signal from the carboxylic acid C=O stretch is very weak.

<sup>b</sup> IR band frequencies and intensities from literature.

<sup>c</sup> Carboxylic acid can be found either as a hydrogen bonded dimer or in the non-hydrogen bonded form.

<sup>d</sup> The aryl and indole ring in-plane vibrations, str. = stretch. The two observed indole in-plane ring vibrations are separate vibrational modes.

approximately 50 cm<sup>-1</sup>. The low-frequency Raman bands of the  $\gamma$ -form of IND are characterized by multiple sharp bands at: 32, 47, 70, 96, 115, 134, and 150 cm<sup>-1</sup>. The FWHH of the four bands below 100 cm<sup>-1</sup> exhibit an average FWHH of 9 cm<sup>-1</sup>; however, our reported FWHH in the low-frequency region is limited by the instrument-grating spectral resolution. The Raman spectrum in general, and the low-frequency spectral region in particular, provides excellent specificity for the crystalline form and good specificity for the amorphous form of IND.<sup>16,18–20</sup> However, the specificity for amorphous IND is better using the broad carbonyl (FWHH of 21 cm<sup>-1</sup>) at 1681 cm<sup>-1</sup> than the broad, asymmetric (FWHH ~50 cm<sup>-1</sup>) amorphous band at 21 cm<sup>-1</sup> in part due to baseline variability below 10 cm<sup>-1</sup>.

The crystallization of amorphous IND at room temperature under laboratory conditions is an excellent example of an unstable amorphous API crystallizing into the more thermodynamically favored crystalline form. By utilizing a single, unperturbed sample of amorphous IND, the transformation to the  $\gamma$ -form was monitored over an eight day period using two spectral regions highlighted in Fig. 3. Figure 4 shows the waterfall plots of the Raman spectra beginning with amorphous IND. The waterfall plots comprising the 1750–1550 cm<sup>-1</sup> and 200–8 cm<sup>-1</sup> Raman spectral regions clearly illustrate the systematic conversion of the amorphous IND to the  $\gamma$ -form. Because of the tenfold greater Raman intensity of the low-frequency bands relative to typical fingerprint bands, both spectral regions are intensity normalized to the strongest crystalline bands at 1699 and 32 cm<sup>-1</sup> to facilitate comparison. In the 1750–1550 cm<sup>-1</sup> spectral region, the amorphous-crystalline IND transformation results in the loss of the broad 1681 cm<sup>-1</sup> benzoyl amide carbonyl band and the steady increase in the sharper crystalline band at 1699 cm<sup>-1</sup>.<sup>16,18–20,23</sup> Changes associated with the aryl indole ring quadrant stretching region are also observed. Most notable is the increase in the band at 1621 cm<sup>-1</sup> in response to the increased relative concentration of the crystalline species over time. In the

low-frequency spectral region between 200–8 cm<sup>-1</sup>, the amorphous-crystalline IND transformation is characterized by the loss of the broad amorphous band at 21 cm<sup>-1</sup> and the formation of the sharp prominent low-frequency crystalline IND bands at 32, 47, 70, 96, and 115 cm<sup>-1</sup>.

The two-dimensional plots of selected Raman band intensity ratios as a function of time provide a more quantitative characterization of the amorphous-crystalline IND transformation. A Raman intensity ratio is employed to correct for typical Raman experimental variability, such as laser power and sample position variability. In general, the peak height analysis of the two components (A, amorphous; C, crystalline) utilize the ratio of the unique bands for component A (or C) divided by the sum of the selected unique bands of the two components (A + C). Thus, assuming no overlapping bands, the completely amorphous material would have a starting value of one for A/(A + C) and zero for C/(A + C). Such an analysis is only semi-quantitative since the peak heights are not scaled to be directly proportional to the analyte concentration. A semi-quantitative analysis is often suitable for many reaction monitoring analyses. A more rigorous quantitative analysis requires scaling factors for both A and C, which is typically determined using well-characterized standards.

The data plot in Fig. 5 utilizes overlapping carbonyl bands, where the crystalline content is calculated using the peak height ratio (Eq. 1) and the amorphous content uses the band height ratio (Eq. 2). Consequently, the amorphous data points (blue) have an initial value at 0.8 rather than 1.0 and convert to 0.2 rather than 0.0. The overlapping carbonyl bands also results in a similar deviation from the ideal zero-to-one plot range for the crystalline data points. A simple band fit analysis could also be employed to eliminate the effect of these overlapping carbonyl bands. Because of the transient nature of amorphous IND, no amorphous-crystalline standards were prepared for a true quantitative analysis. However, the data analysis based upon the carbonyl spectral region provides good signal to noise

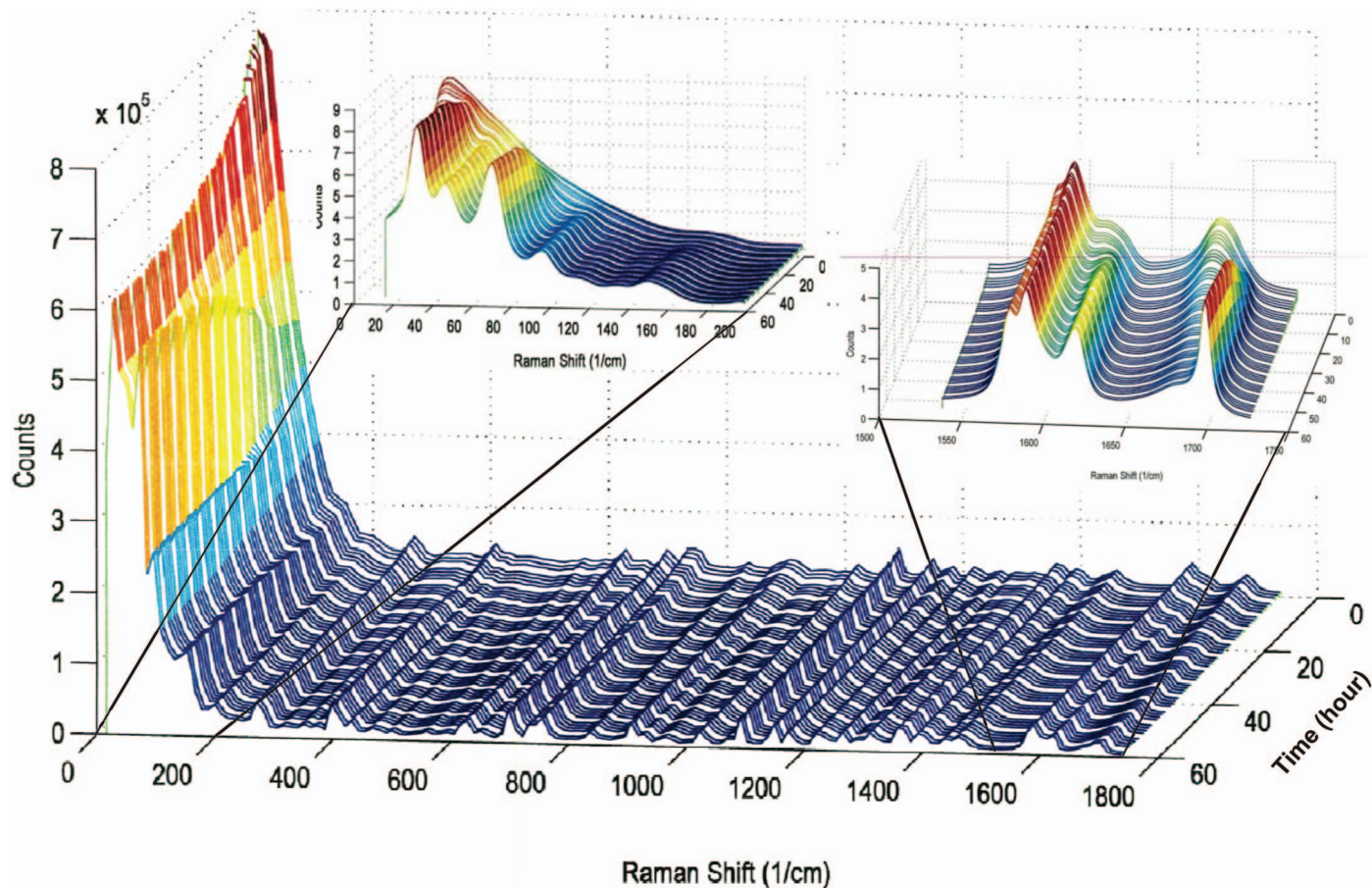


FIG. 4. Raman spectral waterfall plot of the transformation of amorphous IND to the  $\gamma$ -form at room temperature over eight days. The two spectral regions are intensity normalized to the most intense  $\gamma$ -form Raman bands at 1699 and 32  $\text{cm}^{-1}$ . Both intensity axes are included on the waterfall plot associated with the respective spectral region. Displayed sampling rate was every 3 h.

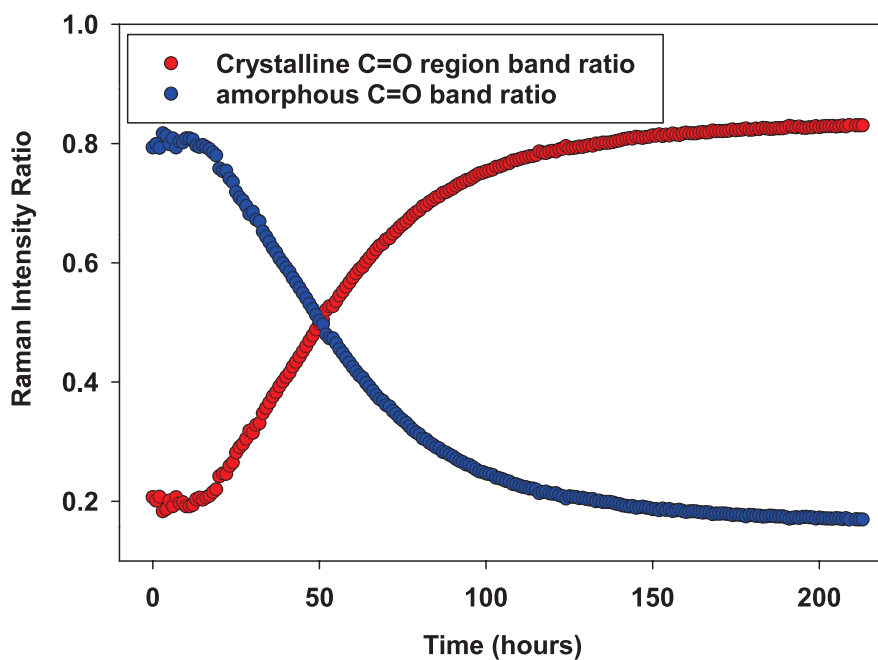


FIG. 5. The time dependence of the amorphous to  $\gamma$ -form conversion of IND monitored using band height Raman intensity ratios. The Raman bands used for analysis included the IND benzoyl amide carbonyl stretching bands for amorphous at 1681  $\text{cm}^{-1}$  and the  $\gamma$ -form at 1699  $\text{cm}^{-1}$ .

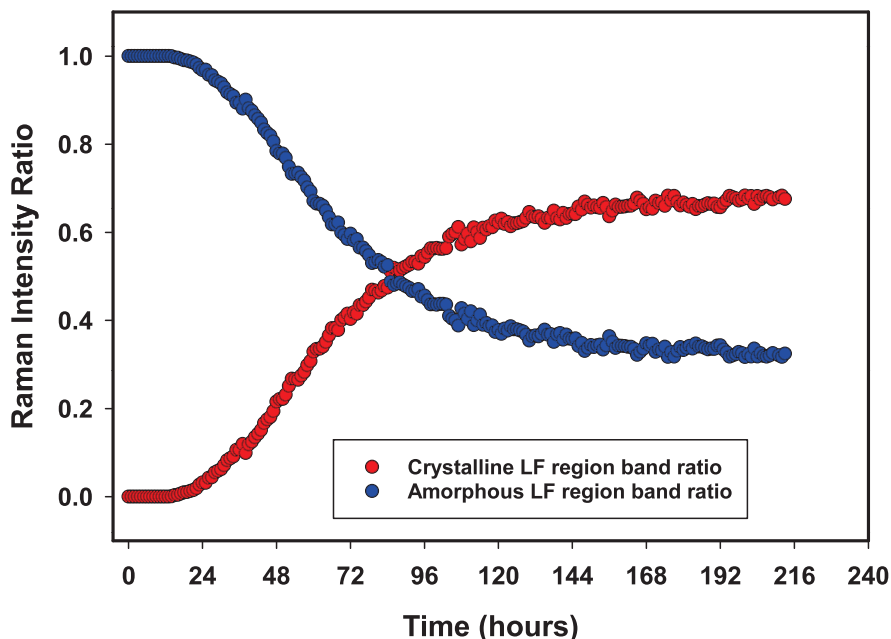


FIG. 6. The time dependence of the amorphous (blue) to  $\gamma$ -form (red) conversion of IND monitored using band height Raman intensity ratios. The low-frequency Raman bands used for analysis included the IND Boson peak for amorphous at  $21\text{ cm}^{-1}$  and the  $\gamma$ -form at  $70\text{ cm}^{-1}$ .

that clearly demonstrates semi-quantitatively the sigmoidal time dependence of the amorphous-crystalline IND conversion.

$$\frac{1699\text{ cm}^{-1}}{1681\text{ cm}^{-1} + 1699\text{ cm}^{-1}} \quad (1)$$

$$\frac{1681\text{ cm}^{-1}}{1681\text{ cm}^{-1} + 1699\text{ cm}^{-1}} \quad (2)$$

The semi-quantitative amorphous-crystalline IND conversion curves shown in Fig. 6 utilize only the low-frequency Raman spectral region. The crystalline content is calculated using the peak height ratio as per Eq. 3, and the amorphous uses the peak height ratio as per Eq. 4. Both show a sigmoidal time dependence and do not include scaling factors to account for the different responses of the amorphous and crystalline components. Here, the amorphous data points (blue), shown in Fig. 6, have an initial value of 1.0 that converts to 0.3 rather than 0.0. The crystalline data points (red) have an initial value of 0.0 that converts to 0.7 rather than 1.0. A local baseline provides a unique isolated peak height with excellent signal-to-noise ratio (SNR) for the crystalline band at  $70\text{ cm}^{-1}$ . The unique isolated band accounts for the plot starting at the ideal values of 1.0 and 0.0 for the amorphous and crystalline ratios, respectively. However, the very broad amorphous band introduces both an overlap and decreased SNR for the low-frequency band height ratio. The observed band intensity variability in the amorphous band occurs due to variation in the local minima baseline point between  $8\text{--}10\text{ cm}^{-1}$ , as well as the superposition of the very broad amorphous band on the sharp crystalline bands below  $150\text{ cm}^{-1}$ . Superior SNR for the low-frequency data is observed

when the  $70\text{ cm}^{-1}$  band is a ratio relative to the  $739\text{ cm}^{-1}$  (not shown).

$$\frac{70\text{ cm}^{-1}}{21\text{ cm}^{-1} + 70\text{ cm}^{-1}} \quad (3)$$

$$\frac{21\text{ cm}^{-1}}{21\text{ cm}^{-1} + 71\text{ cm}^{-1}} \quad (4)$$

The strong, isolated low-frequency Raman bands provide improved sensitivity and specificity for the crystalline component over the carbonyl region.<sup>20</sup> However, the very broad amorphous band provides poorer sensitivity and specificity for the amorphous content compared with the carbonyl region. Figures 5 and 6 demonstrate the effectiveness of Raman spectroscopy to monitor the amorphous to crystalline transformation of IND and the value of including the low-frequency spectral region.

The transformation of amorphous IND to the more stable crystalline form has been used as a model system to investigate the crystallization mechanisms and kinetics using various techniques, including Raman spectroscopy.<sup>18,20,21</sup> Infrared and Raman spectroscopy have established that the IND carboxylic acid group forms a hydrogen bonded dimer between two IND molecules in both the amorphous and crystalline states.<sup>16,23,26</sup> Crystallography has established that the benzoyl carbonyls of adjacent IND molecules are stacked in the unit cell of the  $\gamma$ -form. Both the mid-frequency spectral region between  $1750\text{--}1550\text{ cm}^{-1}$  and the low-frequency region between  $200\text{--}10\text{ cm}^{-1}$  have been used to study the IND crystallization process and kinetics.<sup>20</sup>

The mid-frequency IR and Raman spectral region (between  $1750\text{--}1550\text{ cm}^{-1}$ ) provides information concerning the local environment and the hydrogen bonding

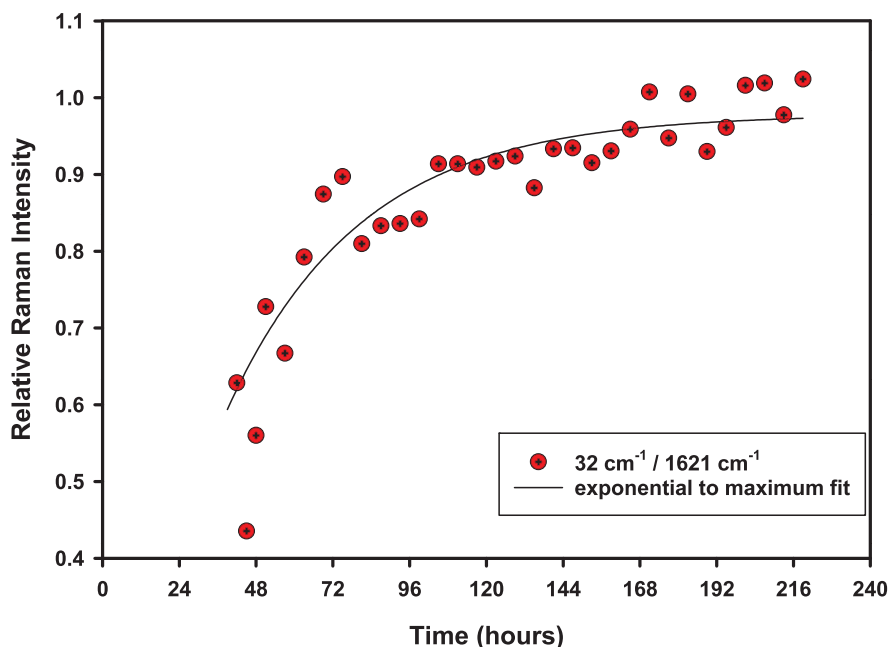


FIG. 7. Scatter plot of the crystalline Raman band ratio  $32/1621\text{ cm}^{-1}$  as a function of time in the amorphous-crystallization transformation of IND to the  $\gamma$ -form. The low-frequency band derives from the long-range phonon vibration, and the mid-frequency band derives from the local crystalline environment of the quadrant ring stretch of the IND aromatic groups.

of the functional groups involved. This includes the very short-range order of the amorphous state and the local interactions of the molecules in the unit cell of the crystal lattice. The low-frequency Raman bands below  $100\text{ cm}^{-1}$  derive mostly from phonon (lattice) vibrations of the crystalline lattice, which thus provide more direct information about the longer-range crystalline environment. The lowest-frequency Raman bands are more likely to be purely phonon vibrational modes.<sup>14</sup> Either of the strong bands at  $70$  and  $32\text{ cm}^{-1}$  can be used to monitor the crystallization of the amorphous material.

Comparison of the Raman intensity of the crystalline bands from low-frequency relative to the mid-frequency regions is another potential tool to gain further insight into API crystallization mechanisms. The same general sigmoidal dependence is observed over time for the amorphous to  $\gamma$ -form IND transformation using both the mid-frequency and low-frequency crystalline Raman bands (see Figs. 5 and 6). This sigmoidal time dependence for the IND crystallization was observed using the carbonyl stretch at  $1699\text{ cm}^{-1}$ , the band involving the ring quadrant stretch at  $1621\text{ cm}^{-1}$ , and the low-frequency phonon vibration at  $32\text{ cm}^{-1}$ . However, the ratio of the mid- and low-frequency Raman bands from the amorphous-crystalline IND transformation is compared; this plot reflects the differences between the short- and long-range type vibrations during crystallization.

Figure 7 shows the Raman area ratio of the  $32\text{ cm}^{-1}$  low-frequency band relative to the  $1621\text{ cm}^{-1}$  aromatic ring stretching vibration as the amorphous IND crystallizes over time. The intensity of the  $1621\text{ cm}^{-1}$  band was multiplied by a factor of 11, normalizing to the intensity to that of the  $32\text{ cm}^{-1}$  band using a fully crystalline IND reference material of the  $\gamma$ -form. The plot clearly shows a non-linear change in the ratio, which plateaus to a

constant value as the IND becomes more crystalline. The  $32/1621\text{ cm}^{-1}$  Raman band area ratio starts well below unity ( $\sim 0.5$ ) at low IND crystallinity and approaches unity as the IND becomes more crystalline after four days. This behavior suggests that, at low crystallinity, where smaller crystalline micro-domains are prevalent, the contribution as monitored by the short-range environmental effects on the aromatic ring vibration ( $1621\text{ cm}^{-1}$ ) is greater than the longer-range crystal lattice vibration. However, as the crystalline lattice becomes more extensive, the intensity of the phonon vibration should reach a constant, maximum intensity that provides a direct, linear probe of the API crystallinity.

Interestingly, the opposite behavior is observed when using the Raman band height ratio of the same  $32\text{ cm}^{-1}$  band relative to the benzoyl carbonyl  $1699\text{ cm}^{-1}$  band. Figure 8 shows the  $32/1699\text{ cm}^{-1}$  Raman band ratio as the amorphous IND crystallizes over time. Once again, the intensity of the  $1699\text{ cm}^{-1}$  benzoyl carbonyl band was multiplied by a factor of 9, normalizing it to the intensity of the  $32\text{ cm}^{-1}$  band using a fully crystalline IND reference material of the  $\gamma$ -form. In this case, the Raman band height ratio at low IND crystallinity is well above one and decreases over four days until it plateaus with a value of approaching one. This suggests that the benzoyl amide carbonyl stretching vibration exhibits less Raman intensity early in the crystallization process.

These results demonstrate that dependence of the Raman intensities of the crystalline bands of IND varies as a function of the extent of crystallization and the particular vibrational mode used. Not surprisingly, systematic differences are observed in the ratio of the low-frequency phonon derived band relative to the mid-frequency Raman bands. The observed behavior of the Raman band intensity involving the benzoyl carbonyl stretch is opposite to that from the aryl-indole ring

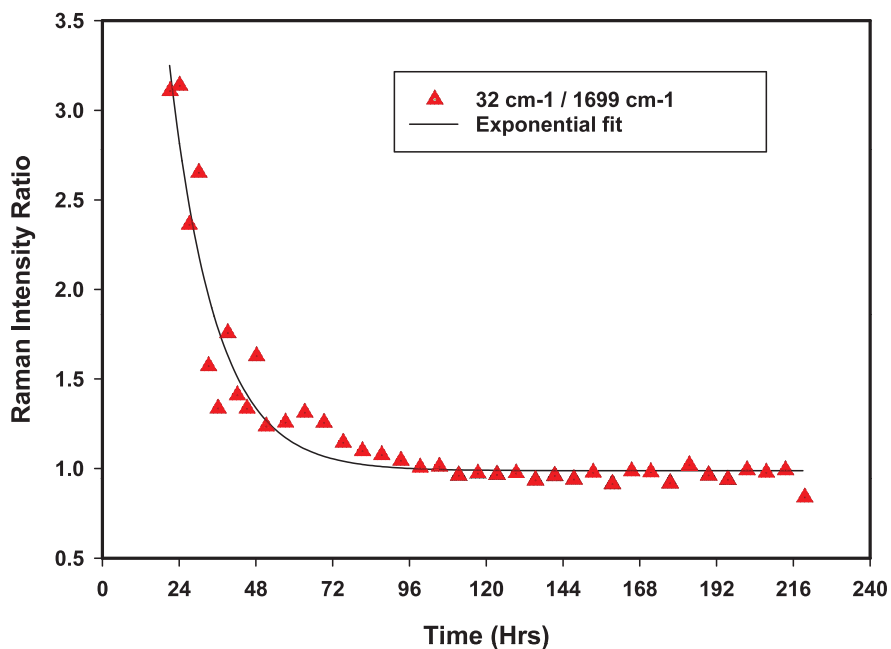


FIG. 8. Scatter plot of the crystalline Raman band ratio  $32/1699\text{ cm}^{-1}$  as a function of time in the amorphous-crystallization transformation of IND to the  $\gamma$ -form. The low-frequency band derives from the long-range phonon vibration, and the mid-frequency band derives from the local crystalline environment of the carbonyl stretch of the benzoyl amide carbonyl group.

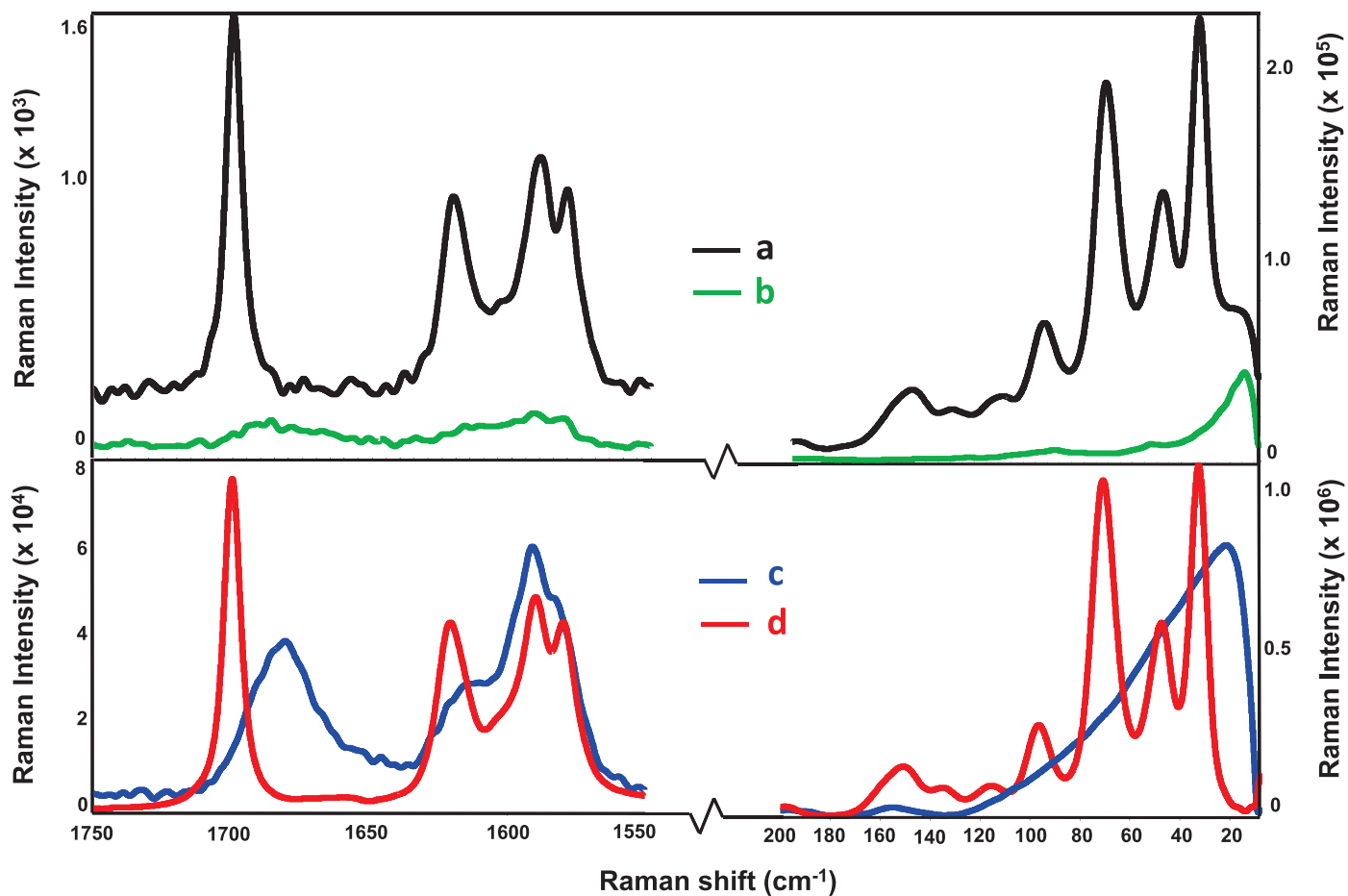


FIG. 9. The Raman spectra in selected regions of indomethacin: (a) black,  $\gamma$ -form suspension at 75 mg/mL in a water-ethanol solvent system, (b) green, fully solubilized in ethanol at 75 mg/mL, (c) blue, in the solid state amorphous form, and (d) red, in the solid-state  $\gamma$ -form. The IND solution and suspension Raman spectra use a common intensity scale to facilitate comparison. The solid-state crystalline and amorphous spectra are intensity normalized to the most intense  $\gamma$ -form Raman bands in the selected mid- and low-frequency spectral regions.

**TABLE II.** Comparison of the benzoyl amide carbonyl stretching Raman band of IND: insoluble  $\gamma$ -form suspension in water-ethanol co-solvent relative to the fully soluble solution in ethanol at the same concentrations.

IND concentration (mg/mL)	C=O stretch $1699\text{ cm}^{-1}$ (suspension)/ $1681\text{ cm}^{-1}$ (solution)	
	Peak height	Peak area
50	12.3	2.2
75	12.4	1.6

quadrant stretching vibration at low crystallinity values. These results suggest that further insight into amorphous-crystalline API transformation mechanisms can be gained by such comparisons of the crystalline Raman band intensities.

**Raman Spectroscopy of Indomethacin in Suspensions and Solution.** Indomethacin is highly soluble in ethanol, but poorly soluble in both water and water-ethanol mixture (50/50 vol%). Ethanol and water-ethanol solvent systems were used to compare the Raman spectra of IND dissolved in solution to that of IND crystalline suspensions at similar concentrations. Figure 9 shows the Raman overlay spectra in the top section of the insoluble suspension of the  $\gamma$ -form of IND (black trace labeled a) and fully dissolved IND solution (green trace labeled b) at the same concentration of 75 mg/mL. Analogous to the previous figures, only a selected mid-frequency region ( $1750\text{--}1550\text{ cm}^{-1}$ ) and low-frequency spectral region ( $200\text{--}10\text{ cm}^{-1}$ ) are shown. However, both spectral regions have their own common intensity scale to facilitate comparison between the solution and suspension IND Raman spectra. The bottom overlay shows the Raman spectra of the solid-state IND in the

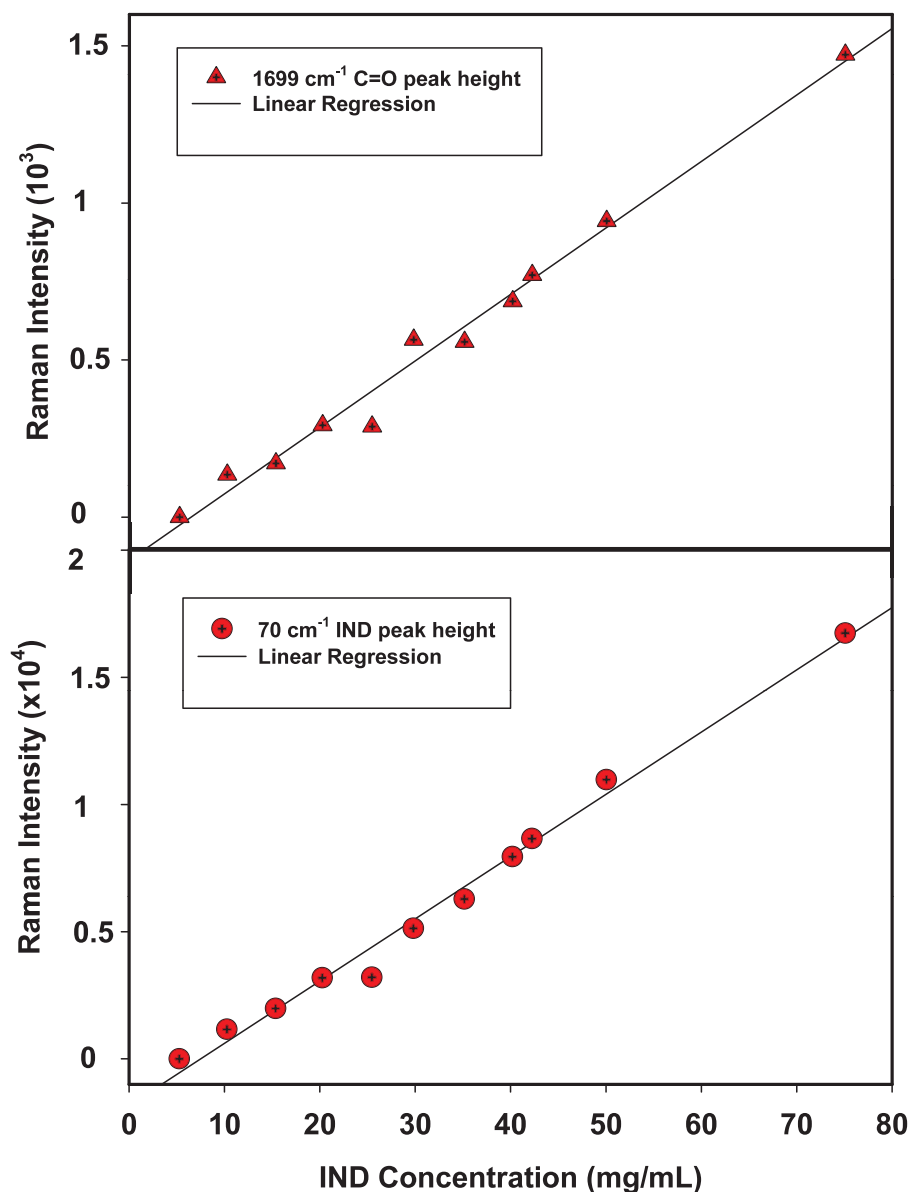


**FIG. 10.** The concentration dependence of a  $\gamma$ -form IND suspension in an insoluble water-ethanol solvent system using the Raman band heights of the  $1699\text{ cm}^{-1}$  carbonyl band and the  $70\text{ cm}^{-1}$  low-frequency band.

amorphous (blue trace, labeled c) and the  $\gamma$ -form (red trace, labeled d). In the bottom spectral overlay, the spectra in each region are normalized using the most intense crystalline Raman bands ( $1699$  and  $32\text{ cm}^{-1}$ ) to facilitate visualization of both spectral regions.

As expected, the Raman spectrum of IND in an ethanol solution is very similar to that of the solid amorphous form while the Raman spectrum of the granular particles of the  $\gamma$ -form in the IND water-ethanol suspension matches that of the solid  $\gamma$ -form. The amorphous and solution Raman spectra of IND exhibit the same broad carbonyl band at  $1681\text{ cm}^{-1}$ , similar features in the  $1640\text{--}1560\text{ cm}^{-1}$  bands, and the same broad asymmetric band below  $120\text{ cm}^{-1}$  deriving from the Boson peak. However, the low-frequency Raman spectra of the IND solution are dominated by contributions from the water-ethanol solvent with only minor contributions from the solution IND.

A qualitative comparison of the Raman spectra of the IND suspension and solution in the carbonyl region in Fig. 9 (trace a and b) can be made since the same concentration is employed ( $75\text{ mg/mL}$ ) along with a common intensity scale. A much greater Raman intensity for the  $\gamma$ -form suspension is clearly observed in comparison to the IND in solution. Some of this behavior for the carbonyl band is due simply from the much narrower FWHH of crystalline IND and the broader FWHH of the IND in solution. A more suitable comparison is to use the areas of the carbonyl bands. Table II summarizes a comparison of both peak heights and peak areas for the Raman carbonyl band intensities of the IND suspension relative to the IND in solution at two different concentrations. The carbonyl peak area comparison for both  $50$  and  $75\text{ mg/mL}$  IND concentrations reveals a twofold increased signal for solid IND suspended particles compared with the same concentration of IND in a transparent solution. This increased Raman intensity for the suspension of IND particles in turbid media most likely derives from multiple scattering phenomena.

Previous work has demonstrated the utility of Raman spectroscopy as an in situ monitor of crystallization from solution.<sup>27,28</sup> The unique crystalline peaks present in both the mid- and low-frequency Raman spectral regions can be used to monitor crystalline IND in a solvent system. Figure 10 plots the peak height intensity of the carbonyl stretching band at  $1699\text{ cm}^{-1}$  and the low-frequency Raman band at  $70\text{ cm}^{-1}$  as a function of the IND suspension weight per volume (milligrams per milliliter). Both bands show a simple linear response of the Raman band intensity as a function of the IND suspension concentration (milligrams per milliliter). The tenfold increased Raman intensity of the low-frequency bands results in a significant increase in sensitivity.

## CONCLUSIONS

This paper highlights the information provided by the low- and mid-frequency Raman spectral regions to study API crystallization using IND as a model system. Both spectral regions provide distinct Raman bands for both the amorphous and crystalline forms of IND. As reported in previous work,<sup>20</sup> the more intense low-frequency Raman bands provide greater sensitivity for detecting

the onset of crystalline formation in an amorphous matrix. Differences in the spectra are observed in the early phase of the API crystallization because the low-frequency region is sensitive to the collective lattice vibrations, while the mid-frequency region is more sensitive to the local environment associated with the functional groups. These results demonstrate that the two spectral regions provide unique probes into the onset of the crystallization process.

The suitability of low-frequency Raman spectroscopy in the monitoring of IND in a suspension was successfully demonstrated. A linear behavior for the Raman band intensities was observed in both the mid- and low-frequency regions as a function of the IND suspension concentration. However, the more intense low-frequency Raman bands provide unique bands for in situ monitoring of crystallization processes. These results suggest that Raman spectroscopy will be a valuable analytical tool for at-line and on-line monitoring of API crystallization.

## ACKNOWLEDGMENTS

We gratefully acknowledge Bristol-Myers Squibb Company and Cytec Industries for providing the resources needed to carry out this paper and for their permission to publish this paper. We also acknowledge both Marta Dabros and Sarah DeLeon of Bristol-Myers Squibb Company for helpful discussions on crystal engineering and PXRD measurements, respectively.

1. S.R. Bryn, R.R. Pfeiffer, J.G. Stowell. "Drugs as Molecular Solids". In: *Solid-State Chemistry of Drugs*. West Lafayette, IN: SSCI, 1999. 2nd ed., Chap. 1. Pp 5-29.
2. S.R. Bryn, R.R. Pfeiffer, J.G. Stowell. "Amorphous Solids". In: *Solid-State Chemistry of Drugs*. West Lafayette, IN: SSCI, 1999. 2nd ed., Chap. 12. Pp 249-258.
3. S.L. Morissette, O. Almarsson, M.L. Peterson, J.F. Remaenar, M.J. Read, A.V. Lemmo, S. Ellis, M.J. Cima, C.R. Gardner. "High-Throughput Crystallization: Polymorphs, Salts, Co-crystals and Solvates of Pharmaceutical Solids". *Adv. Drug Delivery Rev.* 2004. 56: 275-300.
4. A. Burger. "The Relevance of Polymorphism". In: D.D. Breimer, P. Speiser, editors. *Topics in Pharmaceutical Sciences: Proceedings of the International Congress of Pharmaceutical Sciences of FIP held in Vienna, Austria; September 7-11, 1981*. Amsterdam: Elsevier/North Holland Biomedical Press, 1981. Pp 347-359.
5. D.H. Igo, P. Chen. "Vibrational Spectroscopy of Solid-State Forms—Applications and Examples". In: D.E. Pivonka, J.M. Chalmers, P.R. Griffiths, editors. *Applications of Vibrational Spectroscopy in Pharmaceutical Research and Development*. Chichester, UK: John Wiley and Sons, 2007. Pp 293-308.
6. P.J. Larkin. *Infrared and Raman Spectroscopy: Principles and Spectral Interpretation*. New York: Elsevier, 2011.
7. P.J. Larkin, M. Dabros, B. Sarsfield, E. Chan, J.T. Carriere, B.C. Smith. "Polymorph Characterization of Active Pharmaceutical Ingredients (APIs) Using Low-Frequency Raman Spectroscopy". *Appl. Spectrosc.* 2014. 68(7): 758-776.
8. D.E. Bugay, J.O. Henck, M.L. Longmire, F.C. Thorley. "Raman Analysis of Pharmaceuticals". In: D.E. Pivonka, J.M. Chalmers, P.R. Griffiths, editors. *Applications of Vibrational Spectroscopy in Pharmaceutical Research and Development*. Chichester, UK: John Wiley and Sons, 2007. Pp 239-262.
9. D.E. Alonzo, G.G. Zhang, D. Zhou, Y. Gao, L.S. Taylor. "Understanding the behavior of amorphous pharmaceutical systems during dissolution". *Pharm. Res.* 2010. 27(4): 608-618.
10. J. Carriere, R. Heyler, B. Smith. "Polymorph Identification and Analysis Using Ultralow-Frequency Raman Spectroscopy". *Spectroscopy*. 2013. 26(6): S44-S50.
11. E.P.J. Parrott, B.M. Fischer, L.F. Gladden, J.A. Zeitler, P.U. Jepsen. "Terahertz Spectroscopy of Crystalline and Non-Crystalline Solids". In: K.E. Peiponen, A. Zeitler, M. Kuwata-Gonokami, editors.

- Terahertz Spectroscopy and Imaging. Springer Series in Optical Sciences no 171. New York: Springer, 2013. Pp 191-227.
12. M. Born, K. Huang. *Dynamical Theory of Crystal Lattices*. New York: Oxford University Press, 1954.
  13. M. Schwoerer, H.C. Wolf. "Molecular and Lattice Dynamics in Organic Molecular Crystals". In: *Organic Molecular Solids*. Weinheim, Germany: Wiley-VCH, 2007. Chap 5. Pp 89-124.
  14. E.P.J. Parrott, J.A. Zeitler. "Terahertz Time-Domain and Low-Frequency Raman Spectroscopy of Organic Materials". *Appl. Spectrosc.* 2015. 69(1): 1-25.
  15. P.T. Mah, S.J. Fraser, M.E. Reish, T. Rades, K.C. Gordon, C.J. Strachan. "Use of Low-Frequency Raman Spectroscopy and Chemometrics for the Quantification of Crystallinity in Amorphous Griseofulvin Tablets". *Vibrat. Spectrosc.* 2015. 77: 10-16.
  16. L.S. Taylor, G. Zografi. "Spectroscopic Characterization of Interactions Between PVP and Indomethacin in Amorphous Molecular Dispersions". *Pharm. Res.* 1997. 14(12): 1691-1698.
  17. U. Simper, J. Aaltonen, C.M. McGoverin, K.C. Gordon, K. Krauel-Goellner, T. Rades. "Quantification of Process Induced Disorder in Milled Samples Using Different Analytical Techniques". *Pharmaceutics*. 2010. 2(1): 30-49.
  18. J.Y. Kao, C.M. McGoverin, K.A. Graeser, T. Rades, K.C. Gordon. "Measurement of Amorphous Indomethacin Stability with NIR and Raman Spectroscopy". *Vib. Spectrosc.* 2012. 58: 19-26.
  19. L.S. Taylor, G. Zografi. "The Quantitative Analysis of Crystallinity Using FT-Raman Spectroscopy". *Pharm. Res.* 1998. 15(5): 755-761.
  20. A. Hedoux, L. Paccou, Y. Guinet, J. Willart, M. Descamps. "Using the Low-Frequency Raman Spectroscopy to Analyze the Crystallization of Amorphous Indomethacin". *Euro. J. Pharm. Sci.* 2009. 38(2): 156-164.
  21. A. Heinz, M. Savolainen, T. Rades, C.J. Strachan. "Quantifying Ternary Mixtures of Different Solid-State Forms of Indomethacin by Raman and Near-Infrared Spectroscopy". *Euro. J. Pharm. Sci.* 2007. 32(3): 182-192.
  22. A.V. Ewing, G.S. Clarke, S.G. Kazarian. "Stability of Indomethacin with Relevance to the Release Form Amorphous Solid Dispersions Studied with ATR FT-IR Spectroscopic Imaging". *Eur. J. Pharm. Sci.* 2014. 60: 64-71.
  23. C.J. Strachan, T. Rades, K.C. Gordon. "A Theoretical and Spectroscopic Study of  $\gamma$ -Crystalline and Amorphous Indomethacin". *J. Pharm. Pharmacol.* 2007. 59(2): 261-269.
  24. K. Lobmann, R. Laitinen, H. Grohganz, C. Strachan, T. Rades, K.C. Gordon. "A Theoretical and Spectroscopic Study of Co-Amorphous Naproxen and Indomethacin". *Int. J. Pharm.* 2013. 453(1): 80-87.
  25. J. Sibik, K. Löbmann, T. Rades, J.A. Zeitler. "Predicting Crystallization of Amorphous Drugs with Terahertz Spectroscopy". *Mol. Pharm.* 2015. 2(8): 3062-3068.
  26. G. Varsanyi, S. Szoke. *Vibrational Spectra of Benzene Derivatives*. New York: Academic Press, 1969. P. 369.
  27. H. Owen, M. Welch, M.J. Pelletier. *Raman Spectroscopy Crystallization Analysis Method*. US Patent 20040004714 A1 Filed 2003. Issued 2004
  28. A. Hedoux, Y. Guinet, M. Descamps. "The Contribution of Raman Spectroscopy to the Analysis of Phase Transformations in Pharmaceutical Compounds". *Int. J. Pharm.* 2011. 417(1): 17-31.